The Journal of Neuroscience, October 15, 1999, *19*(20):8866–8875

Evidence of Presynaptic Location and Function of the Prion Protein

Jochen Herms,[1] Tobias Tings,[1] Stefan Gall,[1] Axel Madlung,[1] Armin Giese,[1] Heike Siebert,[1] Peter Schürmann,[1] Otto Windl,[1] Nils Brose,[2] and Hans Kretzschmar[1]

[1]*Department of Neuropathology, Georg-August Universität Göttingen, 37075 Göttingen, Germany;* [2]*Max-Planck-Institut für Experimentelle Medizin, 37073 Göttingen, Germany*

The prion protein (PrP^C) is a copper-binding protein of unknown function that plays an important role in the etiology of transmissible spongiform encephalopathies. Using morphological techniques and synaptosomal fractionation methods, we show that PrP^C is predominantly localized to synaptic membranes. Atomic absorption spectroscopy was used to identify PrP^C-related changes in the synaptosomal copper concentration in transgenic mouse lines. The synaptic transmission in the presence of H_2O_2, which is known to be decomposed to highly reactive hydroxyl radicals in the presence of iron or copper and to alter synaptic activity, was studied in these animals. The response of synaptic activity to H_2O_2 was found to correlate with the amount of PrP^C expression in the presynaptic neuron in cerebellar slice preparations from wild-type, $Prnp^{0/0}$, and PrP gene-reconstituted transgenic mice. Thus, our data gives strong evidence for the predominantly synaptic location of PrP^C, its involvement in the regulation of the presynaptic copper concentration, and synaptic activity in defined conditions.

Key words: prion protein; synaptosomes; synaptic transmission; hydrogen peroxide; copper; cerebellum

The prion protein (PrP) is a sialoglycoprotein localized at the cell surface (Stahl et al., 1987). It is mainly expressed in the CNS, particularly in neurons (Kretzschmar et al., 1986; Moser et al., 1995) and to a lesser extent in extraneural tissues (Bendheim et al., 1992; Manson et al., 1992b). In prion diseases, a post-translational modification of the cellular prion protein (PrP^C) leads to the accumulation of an abnormal, conformationally altered isoform, PrP^{Sc} (Prusiner et al., 1996), particularly in the neuropil (Kitamoto et al., 1992).

The localization of PrP^C within neurons, however, is not clear. The majority of immunohistochemical studies describe a somatic expression of PrP^C in neurons with no or only a minor signal in the neuropil (DeArmond et al., 1987; Piccardo et al., 1990; Safar et al., 1990; Bendheim et al., 1992). Data obtained using the histoblot technique (Taraboulos et al., 1992) and electron microscopy (Fournier et al., 1995; Salès et al., 1998), however, indicate a synaptic localization of PrP^C. Moreover, colocalization of PrP^C with the presynaptic vesicle protein synaptophysin was observed, and it has been speculated that PrP^C may be a constituent of the synaptic vesicle membrane or a product stored within vesicles (Fournier et al., 1995). However, the immunoelectron microscopic procedures used in these studies resulted in a destruction of cellular membranes leading to a loss of exact morphological PrP^C location.

Attempts to identify the role of PrP^C in synaptic transmission have yielded controversial results (Collinge et al., 1994; Herms et al., 1995; Manson et al., 1995; Whittington et al., 1995; Lledo et al., 1996). Altered $GABA_A$ receptor-mediated synaptic transmission in the hippocampus of $Prnp^{0/0}$ mice was observed, and postsynaptic mechanisms were implicated (Collinge et al., 1994). Outside-out membrane patches of cerebellar Purkinje cells, however, did not reveal any alteration of the $GABA_A$ receptor in $Prnp^{0/0}$ mice (Herms et al., 1995). Also, the described alteration in the rise time of IPSCs in hippocampal CA1 neurons (Collinge et al., 1994) could not be reproduced in either cerebellar Purkinje cells (Herms et al., 1995) or hippocampal CA1 neurons (Lledo et al., 1996).

In this study, we used synaptosomal fractionation methods to determine the subcellular neuronal localization of PrP^C. These analyses were complemented by a more detailed morphological investigation of PrP^C expression using immunohistochemical techniques. Our results support the notion that PrP^C is predominantly expressed at the presynaptic membrane. Because PrP^C is known to bind copper, we used atomic absorption spectroscopy to show a reduction in the copper concentration in synaptosomal preparations of $Prnp^{0/0}$ mice.

For a functional analysis of PrP^C and the copper concentration at the presynapse, we performed patch-clamp measurements on cerebellar slice preparations of wild-type, $Prnp^{0/0}$, and PrP-reconstituted transgenic mice. For these experiments, we used hydrogen peroxide, which is known to alter synaptic vesicle release by reacting with metal ions, such as iron and copper at the presynapse (Pellmar et al., 1994), by increasing the presynaptic calcium concentration. Using transgenic lines that express PrP^C in anatomically defined neurons, we observed that the effect of H_2O_2 on the frequency of spontaneous IPSCs (sIPSCs) in cerebellar Purkinje cells correlates with the amount of PrP^C expressed in the presynaptic neuron.

Thus, our data show that PrP^C is localized to the synaptic membrane and that PrP^C is involved in regulating the presynaptic copper concentration and synaptic transmission under biochemically defined conditions.

MATERIALS AND METHODS

Experimental animals. The animals used for these experiments were $Prnp^{0/0}$ mice (Büeler et al., 1992) and wild-type C57Bl/6J×129/sv(ev)

Received May 27, 1999; revised July 26, 1999; accepted July 30, 1999.

This work was supported by BMBF (German Federal Ministry of Science and Technology) Grant KI 9461/8, Wilhelm-Sander-Stiftung Grant 9343008, and Deutsche Forschungsgemeinschaft Grant KR 1561/2–1 and Sonderforschungsbereich 406. We thank Charles Weissmann (University of Zürich) for $Prnp^{0/0}$, tg35, and tg20 mice, Dr. Christophe Pouzat for the program for analysis of synaptic activity, and Dr. Bernhard Keller for helpful comments on this manuscript.

Correspondence should be addressed to Dr. H. A. Kretzschmar, Georg-August Universität Göttingen, Robert-Koch-Strasse 40, 37075 Göttingen, Germany.

hybrids. Also included in the analysis were mice overexpressing the mouse Prnp-b allele (tg35) and the mouse Prnp-a allele (tg20) on a $Prnp^{0/0}$ background, as described previously (Fischer et al., 1996).

Subcellular fractionation. Synaptic plasma membranes (SPMs), synaptic vesicle (SV) fractions, and cytosolic synaptosomal (CS) fractions were prepared following standard protocols (Huttner et al., 1983; Brose et al., 1989). All procedures were performed at 4°C. Twenty brains of adult wild-type, $Prnp^{0/0}$, and tg35 mice were collected in 80 ml of ice-cold 0.32 M sucrose and homogenized using a glass–Teflon homogenizer. The resulting homogenate was centrifuged at 800 × *g* for 10 min. The supernatant was pelleted again at 9200 × *g* for 15 min. The resulting crude synaptosomal pellet was washed by resuspension and recentrifugation (9200 × *g* for 15 min), resuspended in 15 ml of 0.32 M sucrose, and homogenized in 9 vol of H_2O containing 0.2 mM PMSF, 0.5 μg/ml leupeptin, and 1 μM pepstatin. The suspension was stirred at 4°C for 15 min. Centrifugation at 25,000 × *g* for 20 min produced a pellet with lysed synaptosomal membranes. After ultracentrifugation of the supernatant at 230,000 × *g* for 2 hr, the supernatant contained the CS fraction, and the pellet contained the crude SV fraction. The lysed synaptosomal membrane fraction was resuspended in 5 ml of H_2O and loaded on a sucrose density gradient containing 15 ml of 1.2 M sucrose, 15 ml of 0.8 M sucrose, and 5 ml of 0.3 M sucrose. After centrifugation at 113,000 × *g* for 150 min in a Beckman Instruments (Fullerton, CA) SW 28 rotor, the SPM fraction band between 0.8 and 1.2 M sucrose was collected.

Postsynaptic densities. Triton X-100 was used to separate postsynaptic densities (PSDs) from other synaptic elements based on insolubility in the detergent (Carlin et al., 1980). The prepared crude synaptosomal fraction was resuspended in buffer B (0.32 M sucrose and 1 mM $NaHCO_3$) and loaded onto a sucrose density gradient containing 15 ml each of 1.4 and 1.0 M sucrose. After centrifugation at 82,500 × *g* for 60 min in a Beckman SW 28 rotor, the band between 1.4 and 1.0 sucrose was collected and diluted in buffer B to a final concentration of 4 mg/ml. After adding an equal volume of 1% (v/v) Triton X-100, the suspension was stirred for 15 min at 4°C and centrifuged at 32,800 × *g* for 10 min. The resulting pellet was resuspended in buffer B and loaded on another sucrose density gradient containing 4 ml of 2.0 M sucrose, 3 ml of 1.5 M sucrose and 3 ml of 1.0 M sucrose. After centrifugation at 201,800 × *g* for 120 min in the Beckman SW 40 rotor, the PSD fraction band between 1.5 and 2.0 M sucrose was collected, diluted in buffer B to a volume of 9 ml, mixed with an equal volume of 1% Triton X-100 in 150 mM KCl, loaded onto a further sucrose density gradient containing 1.5 ml each of 2.1 and 1.5 M sucrose, and spun at 113,000 × *g* for 10 min using the Beckmann SW 40 rotor. This procedure was repeated once. The PSD band was diluted in HEPES–KOH and pelleted at 113,500 × *g* for 10 min. The resulting pellet containing PSDs was collected in HEPES–KOH buffer.

Preparation of synaptosomes. Synaptosomes were prepared by a modification of the procedure of Nicholls (McMahon et al., 1992). Five brains, excluding brainstem of female, 2-month-old wild-type, $Prnp^{0/0}$, and tg20 mice were collected in 30 ml of ice-cold 0.32 M sucrose and homogenized using a glass–Teflon homogenizer. The resulting homogenate was centrifuged at 3440 × *g* for 2 min. The supernatant was pelleted again at 16,700 × *g* for 12 min. The resulting crude synaptosomal pellet was resuspended in 4 ml of 0.32 M sucrose and put on a three-step Ficoll (Amersham Pharmacia Biotech, München, Germany) gradient (6, 9, and 13%). After centrifugation at 64,000 × *g* for 35 min, the interfaces were collected and pooled. The integrity of the synaptosomes was confirmed by electron microscopy.

Atomic absorption spectroscopy. Synaptosomes were dried at 150°C overnight and ashed at low temperature for 24 hr using plasma processor TePLa 100-e (Technics Plasma). The residue was absorbed in nitric acid. Cu measurements were performed using a Zeeman 3030 (Perkin-Elmer, Emeryville, CA) flameless atomic absorption spectrophotometer at a wavelength of 325.2 nm after rapid atomization at 2000°C in a graphite-tube cuvette HGA-70 (Perkin-Elmer).

Antibodies. Murine PrP^C was detected using either a rabbit antiserum (Ra5) raised against a synthetic peptide corresponding to amino acid residues 107–122 (Groschup et al., 1994) or the monoclonal antibody 3B5 raised by DNA-mediated immunization of $Prnp^{0/0}$ mice and mapped to amino acids 54–69 of human PrP (Krasemann et al., 1996). Polyclonal antibodies to synaptotagmin I (Perin et al., 1990) were a gift from T. C. Südhof (Dallas, TX). Monoclonal antibodies to NMDA-R1 were raised against a fusion protein of NMDA-R1 with glutathione *S*-transferase (Brose et al., 1994).

SDS-PAGE and Western blot analysis. Protein samples were quantified by standard procedures (BCA Protein Assay; Sigma, Deisenhofen, Germany) with bovine serum albumin as a standard. SDS-PAGE was performed using either 10 or 15% gels. Proteins were transferred to a nitrocellulose membrane (Schleicher & Schuell, Göttingen, Germany) using a semi-dry electrotransfer system (Phase, Lübeck, Germany). The blots were blocked with 0.2% I-Block (Tropix, Bedford, MA) in PBS–0.1% Tween 20 for 30 min and were then incubated with primary antibodies for 1 hr at room temperature, followed by an incubation with alkaline phosphatase (AP)-conjugated goat anti-rabbit or anti-mouse antibodies from Dako (Hamburg, Germany) (1:500) for 1 hr at room temperature. After the incubation steps, the membranes were washed with PBS–0.1% Tween 20. Immunopositive signals were detected using the chemiluminescent substrate CDP-StarTM (Tropix) following the manufacturer's instructions. The light signals were monitored, documented, and quantified using a CCD-video system and the accompanying software (Raytest, Straubenhardt, Germany). Blots were developed using nitroblue-tetrazolium-chloride (NBT) and 5-brom-4-chlor-indolylphosphate (BCIP) (Boehringer Mannheim, Mannheim, Germany).

Immunohistochemistry of cryostat sections. Animals were killed by an overdose of 7% chloral hydrate, and their eyes were immediately removed from the sockets. The eyes were mounted in Tissue Tek (OCT compound; Miles Inc., Elkhart, IN) and rapidly frozen in precooled isopentane; the same procedure was performed for the brain after removal from the skull. The samples were kept at −80°C until sectioning. Sections of 8 μm thickness were made at −20°C, air-dried, fixed in ethanol for 10 min, and kept at −20°C. Frozen sections were thawed, rinsed in 0.1 PBS, pH 7.4, and blocked with 2% bovine serum albumin. The sections were incubated with an undiluted medium supernatant containing the monoclonal antibody 3B5. After rinsing, the slides were incubated with a fluorescent goat anti-mouse antibody (Oregon Green 488; 1:200; Molecular Probes, Eugene, OR). For synaptophysin immunohistochemistry, sections were treated as described above and incubated overnight with a monoclonal antibody against synaptophysin (1:10; Boehringer Mannheim). A tetramethylrhodamine isothiocyanate-coupled goat anti-mouse IgG was used as a secondary antibody (1:200; Dianova, Hamburg, Germany). Sections were examined using the Leica (Heidelberg, Germany) TCS NT laser scanning system mounted on an Olympus Opticals (Tokyo, Japan) BX50 WI microscope.

Histoblots. Histoblots for the detection of PrP^C were performed using a modification of the method described previously (Taraboulos et al., 1992). Sections of frozen brain tissue were cut at 10 μm and immediately transferred onto nitrocellulose membranes that had been wetted in lysis buffer (0.5% NP-40, 0.5% sodium desoxycholate, 100 mM NaCl, 10 mM EDTA, and 10 mM Tris-HCl, pH 7.8). The membranes were air-dried thoroughly and rehydrated for 1 hr in TBST-buffer (100 mM NaCl, 0.05% Tween 20, and 10 mM Tris-HCl, pH 7.8). Blots were rinsed three times in TBST, then blocked with 5% nonfat dry milk, rinsed in TBST again, and incubated for 12 hr at 4°C with antiserum Ra5 in TBST and 1% nonfat milk. Rabbit antiserum was used at a dilution of 1:500. Secondary goat anti-rabbit AP-conjugated antibody (Dako) was used at a dilution of 1:1000 in TBST and 1% nonfat milk. Blots were developed using NBT and BCIP (Boehringer Mannheim).

Whole-cell voltage-clamp recordings of cerebellar Purkinje cells. Patch-clamp experiments were performed on Purkinje cells in thin slices of the cerebellum following standard procedures (Hamill et al., 1981; Edwards et al., 1989). Sagittal slices of cerebellum (150 μm) were prepared from 9- to 13-d-old mice as described previously (Edwards et al., 1989; Herms et al., 1995) and maintained at 37°C in a continuously bubbled (95% O_2 and 5% CO_2) solution (125 mM NaCl, 2.5 mM KCl, 1.25 mM NaH_2PO_4, 26 mM $NaHCO_3$, 2 mM $CaCl_2$, 1 mM $MgCl_2$, and 25 mM glucose). After 60 min recovery, the slices were placed in the recording chamber and superfused with the above solution at room temperature. A Purkinje cell was selected using an upright microscope with a 63× water-immersion lens (Zeiss, Göttingen, Germany). Electrodes were pulled from borosilicate glass capillaries and filled with a solution containing (in mM 140 CsCl, 10 HEPES, 10 EGTA, 1 $CaCl_2$, 2 $MgCl_2$, 4 Na_2-ATP, and 0.4 Na_3-GTP (adjusted to pH 7.3 with CsOH). Single-electrode voltage-clamp recordings (Edwards et al., 1989) were performed with a patch-clamp amplifier (EPC-9; Heka Elektronik, Lambrecht, Germany) using optimal series resistance compensation as recommended (Llano et al., 1991). The whole-cell capacitance and series resistance (R_s) adjustment of the amplifier were used to compensate the initial portion of the capacitance transient elicited by 10 mV hyperpolarizing pulses and to estimate the value of the series resistance (Llano et al., 1991). The series resistance of Purkinje cells before compensation was typically 3–10 MΩ. No significant differences were observed here between the different

transgenes studied and wild-type Purkinje cells. Series-resistance compensation was set at between 60 and 70%. R_s was monitored throughout the experiments by hyperpolarizing pulses applied every 30 sec. The experiment was discontinued if the series resistance increased above 15 MΩ or >20% of the initial value. Our results are derived from a data set of 96 Purkinje cells.

H_2O_2 was diluted daily from a 30% stock solution and applied by bath perfusion. Given the perfusion rate of 1.0–1.5 ml/min and the volume of 1.1 ml of the chamber, exchange of the external solution was achieved within a very short time. The bath solutions contained 10 μM of the antagonist of ionotropic glutamate receptors 6-cyano-7-nitroquinoxaline-2,3-dione, as well as in some experiments 0.5 μM tetrodotoxin (TTX) purchased from Biotrend (Köln, Germany). All other chemicals used were purchased from Sigma.

RESULTS

Detection of PrP^C in histoblots

Histoblots of brain sections from wild-type and PrP^C-overexpressing mice (tg35) were immunostained to analyze the pattern of PrP^C expression. Only a very weak, non-definitive signal was detected in wild-type mice (Fig. 1*A*). No signal was seen in $Prnp^{0/0}$ mice, which served as negative controls (Fig. 1*B*). However, strong staining was seen on brain sections from tg35 mice overexpressing PrP^C (Fig. 1*C*). In these mice, strong staining was found in regions of high synaptic density, i.e., in hippocampal stratum oriens, stratum radiatum, stratum lacunosum moleculare (Fig. 1*D*), and in the molecular layer of the cerebellum (Fig. 1*F*). The signal was absent in regions primarily consisting of nerve cell somata, i.e., in the granular layer of the hippocampal dentate gyrus and the stratum pyramidale of the hippocampal CA1 region (Fig. 1*E*, hematoxilin–eosin stain of a parallel section). Intermediate-to-faint staining was observed in the cerebral cortex and other gray matter regions without localization to specific cortical regions or layers.

Localization of PrP^C in mouse cerebellum and retina of transgenic animals

Further immunohistochemical examination using confocal laser microscopy revealed highest expression of PrP^C in the cerebellar molecular layer in both tg20 mice and tg35 mice (Fig. 2*A*,*B*). Here, PrP^C was found to be coexpressed with synaptophysin (data not shown). In tg35 mice, the Purkinje cell bodies also showed immunoreactivity, whereas in tg20 mice, we observed no signal in the Purkinje cell layer (Fig. 2*B*), consistent with the finding that tg20 Purkinje cells do not express PrP^C (Fischer et al., 1996).

Both transgenic lines showed strong immunoreactivity in the molecular layer, which is primarily composed of granule cell axons (parallel fibers) and Purkinje cell dendrites. Because Purkinje cells of tg20 mice do not express PrP^C, the strong PrP^C immunoreactivity in the molecular layer of these animals does not originate from the Purkinje cell dendrites, but mostly from granule cell axons.

No signal was detected in wild-type retina (Fig. 2*C*). Within the retina of a transgenic line overexpressing PrP^C (tg20), immunohistochemistry revealed strong staining in the inner and outer plexiform layers (Fig. 2*D*), which are regions of high synaptic density, as shown by synaptophysin immunohistochemistry (Fig. 2*E*). There was only low immunoreactivity in the internal or external granule cell layers. Very low PrP^C immunoreactivity was observed in the inner segments of the photoreceptor cells. No PrP^C immunopositivity was detected in the outer segments. Figure 2*F* clearly shows that PrP^C is colocated with the synaptic protein synaptophysin.

Preferential localization of PrP^C in the synaptic membrane fraction

Biochemical preparation of subcellular fractions of wild-type mice and PrP^C-overexpressing mice was used to more clearly define the localization of PrP^C in wild-type neurons and to compare these with PrP^C-overexpressing neurons. Whole-brain homogenates, crude SV fractions, CS fractions, and SPM fractions from adult mice were isolated. The synaptic plasma membrane fraction from $Prnp^{0/0}$ mice served as control. Using the antibody 3B5 (Fig. 3*A*,*C*) and the antiserum Ra5 (Fig. 3*B*), we observed a strong PrP^C signal in the SPM fraction in wild-type mice (Fig. 3*A*,*B*) and in tg35 (Fig. 3*C*). The two main glycosylated forms (33–35 and 30 kDa) and one unglycosylated form (27 kDa) of PrP^C were clearly distinguishable. A small band was seen in the SPM fraction of $Prnp^{0/0}$ mice (Fig. 3*A*), which was unspecific because it was not detectable in the blot probed with a different PrP antibody (Fig. 3*B*). PrP^C was also detected in the crude synaptic vesicle fraction in both wild-type and PrP^C-overexpressing mice (Fig. 3*A–C*, *SV*). In contrast to the synaptic vesicle protein synaptotagmin (Fig. 3*D*), there was a stronger band of PrP^C in the SPM fraction than in the crude synaptic vesicle fraction (Fig. 3*A–C*). Neither synaptotagmin nor PrP^C were detected in the CS fraction (Fig. 3*A–D*). A comparison of the PrP^C signal of the brain homogenate with the PrP^C signal from the SPM fraction showed an enrichment factor of 3 to 4 in both wild-type mice and PrP^C-overexpressing mice. As shown in a Western blot with an antibody directed against NMDA receptor subunit 1, the synaptic vesicle fraction is not pure (Fig. 3*E*). Although these results show that the major amount of PrP^C is localized to the synaptic plasma membrane, it remains unclear what proportion of PrP^C is in the synaptic vesicle fraction.

To address the subcellular localization of PrP^C in synapses more directly, we quantified the relative amounts of PrP^C on the cell surface and on transport–synaptic vesicles. For that purpose, we isolated Ficoll-purified synaptosomes and treated these with trypsin. This treatment should lead to complete degradation of the cell surface–plasma membrane pool of PrP^C but leave intracellular vesicular pools unaffected. We found that trypsin digestion of Ficoll-purified synaptosomes leads to complete degradation of all detectable synaptosomal PrP^C, indicating that very little or no PrP^C is present on synaptic vesicles. In contrast, the synaptic vesicle protein synaptotagmin remained intact under these conditions (data not shown). This finding further supports the notion that PrP^C is located predominantly on the synaptic plasma membrane rather than on the synaptic vesicle membrane, as proposed by Fournier et al. (1995).

For a clearer location of PrP^C at the presynaptic or postsynaptic membrane, we isolated PSDs. In contrast to the NMDA receptor subunit 1 (Fig. 3*G*), a protein known to be present in this fraction, PrP^C was not detected in the postsynaptic density fraction of wild-type mice (Fig. 3*F*, using the Ra5 PrP antibody as in *B*).

Copper concentration in synaptosomes is related to PrP^C

A strong correlation of the prion protein expression and the copper content of crude membrane-enriched fractions from brain homogenates has been described previously (Brown et al., 1997a). Whole-brain homogenates, however, do not show any significant difference in the copper content between wild-type, $Prnp^{0/0}$, and PrP^C-overexpressing mice (Fig. 4*A*). However, differences were observed in synaptosomal preparations, fractions in which PrP^C is enriched (Fig. 4*B*). Here, the copper concentration was signifi-

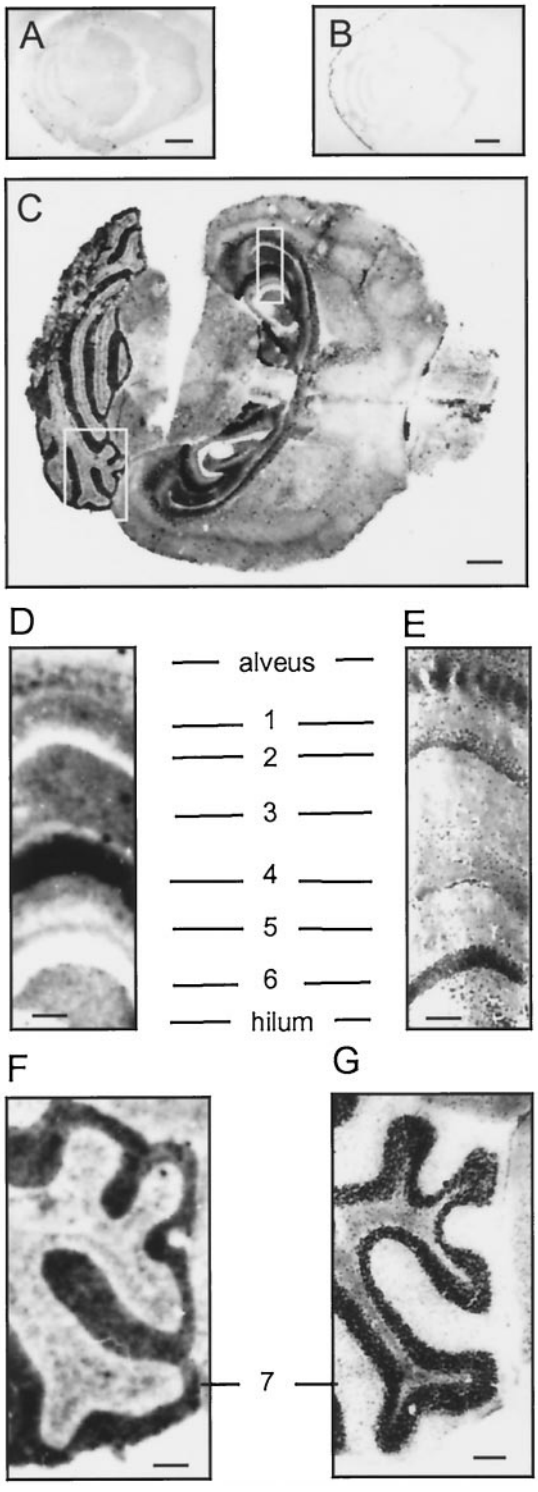

Figure 1. PrP^C is preferentially localized to areas of high synaptic density. Histoblots of wild-type (*A*), $Prnp^{0/0}$ (*B*), and PrP^C-overexpressing reconstituted $Prnp^{0/0}$ (tg35) (*C*) mice. The blots were probed with anti-PrP antiserum Ra5. No PrP^C was detected in $Prnp^{0/0}$ mice (*B*) or in wild-type mouse brains (*A*). *D* and *F* show enlargements from *boxes* in *C*. *E* and *G* show consecutive hematoxilin and eosin stains. *D*, *E*, PrP^C is strongly expressed in areas of high synaptic density of the hippocampal stratum orients (*1*), stratum radiatum (*3*), stratum lacunosum moleculare (*4*), and the molecular layer (*5*). No signal was detected in the hippocampal pyramidal cell layer (*2*) or the granular layer of the dentate gyrus (*6*). *F*, *G*, High PrP^C expression in the cerebellar molecular layer (*7*). Scale bars: *A*, 1 mm; *B*, *C*, 2.5 mm; *D–G*, 250 μm.

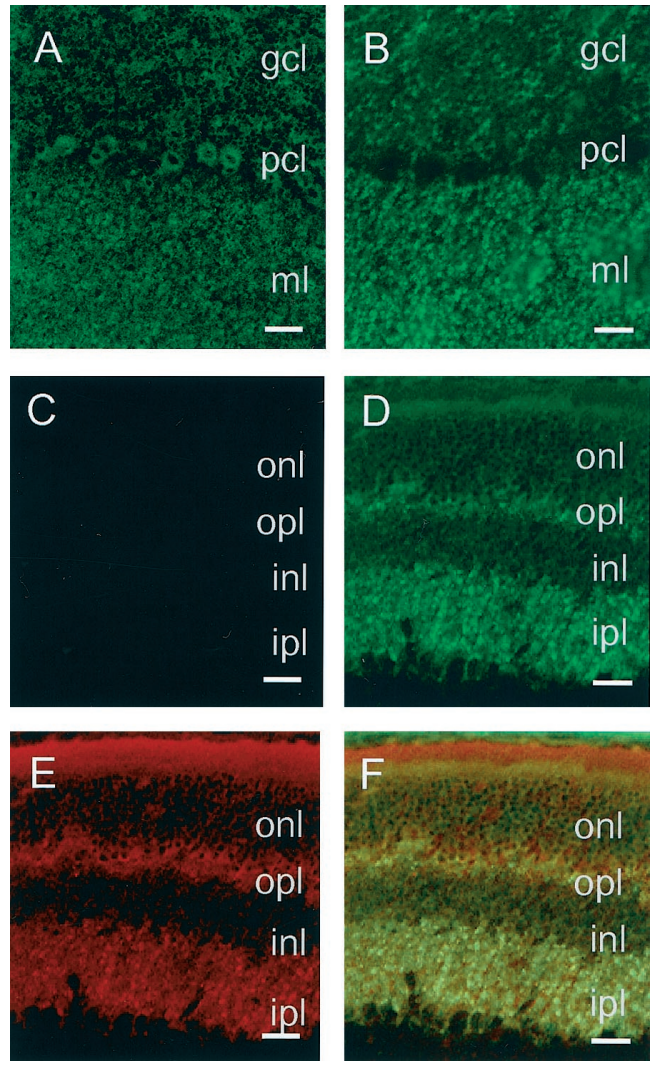

Figure 2. Laser scanning confocal images of PrP^C in the cerebellar cortex and retina of wild-type and PrP^C-overexpressing $Prnp^{0/0}$-reconstituted mice. *A*, *B*, Cerebellar cortex of tg35 and tg20 animals analyzed using PrP antibody 3B5. In tg35 (*A*), PrP^C was detected over the granule cell layer (*gcl*), the Purkinje cell bodies (*pcl*), and the molecular layer (*ml*). In tg20 (*B*), a strong PrP^C expression was observed over the molecular layer and granule cell layer but not in the Purkinje cell layer. *C–F*, Retina of wild-type (C) and PrP^C-overexpressing tg20 (*D–F*) mice. Using PrP antibody 3B5, no signal was detected in wild-type mice (*C*), whereas the tg20 retina (*D*) showed a strong PrP^C expression in the inner plexiform layer (*ipl*), as well as the outer plexiform layer (*opl*). In tg20 mice, synaptophysin (*E*) was found to be coexpressed with PrP^C in the outer and inner plexiform layers (*F*). PrP^C expression is low in the outer (*onl*) and inner nuclear layers (*inl*). Scale bars: *A–F*, 150 μm.

cantly lower in $Prnp^{0/0}$ (23 ± 6 ng of Cu/mg of protein) than in wild-type mouse preparations (39 ± 9 ng of Cu/mg of protein). In tg20 mice, which overexpress PrP^C on a $Prnp^{0/0}$ background, the copper concentration was found to be in the same range as in wild-type animals (40 ± 13 ng of Cu/mg of protein).

Effect of hydrogen peroxide on inhibitory synaptic transmission in wild-type, $Prnp^{0/0}$, and PrP^C-overexpressing mice

Biochemical investigation has shown a predominant location of PrP^C at the synaptic plasma membrane, and atomic absorption measurements have revealed that synaptosomal copper concen-

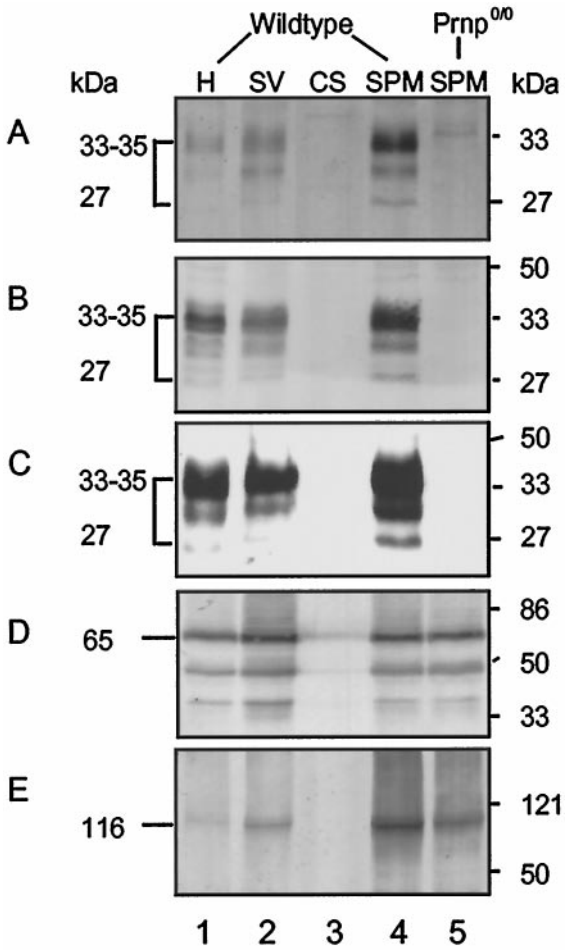

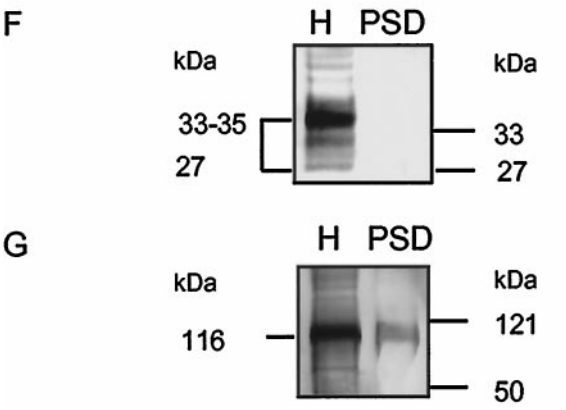

Figure 3. Enrichment of PrP^C in the synaptic plasma membrane fraction but not in the postsynaptic density fraction isolated from mouse brains. Equal amounts (100 μg/lane) of subcellular fractions from wild-type mouse brain and prion protein-deficient mouse brain ($Prnp^{0/0}$) were analyzed by immunoblotting with anti-PrP antibody 3B5 (*A*) and antiserum Ra5 (*B*). For comparison, subcellular fractions of PrP^C-overexpressing tg 35 mice (30 μg/lane) were also examined using antibody Ra5 (*C*). The immunostaining for synaptotagmin (*D*) and NMDA receptor subunit NMDA-R1 (*E*) was used as a control for synaptic vesicle proteins and postsynaptic membrane proteins, respectively. Subcellular fractions are designated as follows: *H*, homogenate; *SV*, crude synaptic vesicle fraction; *CS*, cytosolic synaptosomal fraction; *SPM*, synaptic plasma membranes. *F*, In the PSD fraction, PrP^C is not detectable (Western blot analysis in homogenates and PSD with antibody 3B5; 30 μg of protein were loaded in each lane). *G*, Immunostaining for NMDA-R1 was used as a control for postsynaptic membrane proteins.

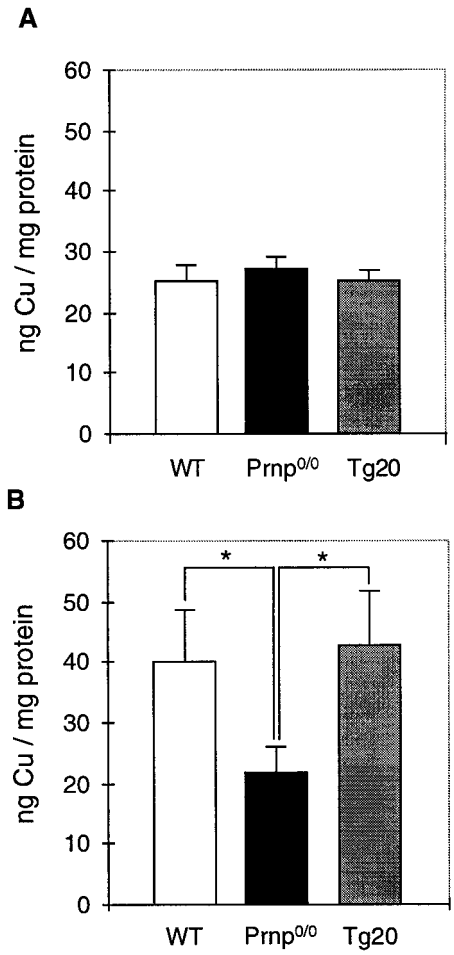

Figure 4. Copper concentration in synaptosomes correlates with PrP^C expression. The copper concentration in whole-brain homogenates (*A*) and synaptosomal fractions (*B*) of wild-type (*WT*), $Prnp^{0/0}$, and Prnp-reconstituted $Prnp^{0/0}$ mice (tg20) was studied by atomic absorption spectroscopy. The copper concentration was not significantly different in the whole-brain homogenates of the three lines tested. The synaptosomal preparations reveal a significantly reduced copper concentration in $Prnp^{0/0}$ mice compared with wild-type mice (Student's *t* test; $p < 0.05$). In PrP^C gene-reconstituted $Prnp^{0/0}$ mice (tg20), the synaptosomal copper concentration was similar to wild-type mice. Shown are the mean and SE for four to six independent preparations of five age- and sex-matched brains. *Asterisks* indicate that the observed differences were found to be statistically significant.

tration is related to PrP^C. Copper binding by PrP^C may therefore have functional consequences for synaptic transmission (Brown et al., 1997a). Here, we studied the effect of hydrogen peroxide, which is known to react with metal ions such as copper to form highly reactive oxygen species. These have been shown to modulate synaptic transmission predominantly on a presynaptic level (Gilman et al., 1992; Palmeira et al., 1993; Pellmar et al., 1994; Pellmar, 1995).

Figure 5 illustrates the effect of 0.01% H_2O_2 on the inhibitory synaptic activity of a Purkinje cell in wild-type (*A–G*) and $Prnp^{0/0}$ (*H–N*) mice. *A* and *H* display a sample of a continuous recording of sIPSCs in control saline 5 min before the application of H_2O_2, as indicated in Figure 5, *C* and *J*. Spontaneous IPSCs were recorded as inward currents because of the fact that the Nernst equilibrium potential for Cl^- ions is close to 0 mV. *B* and *I* correspond to samples of sIPSCs taken from the same cells 8 min

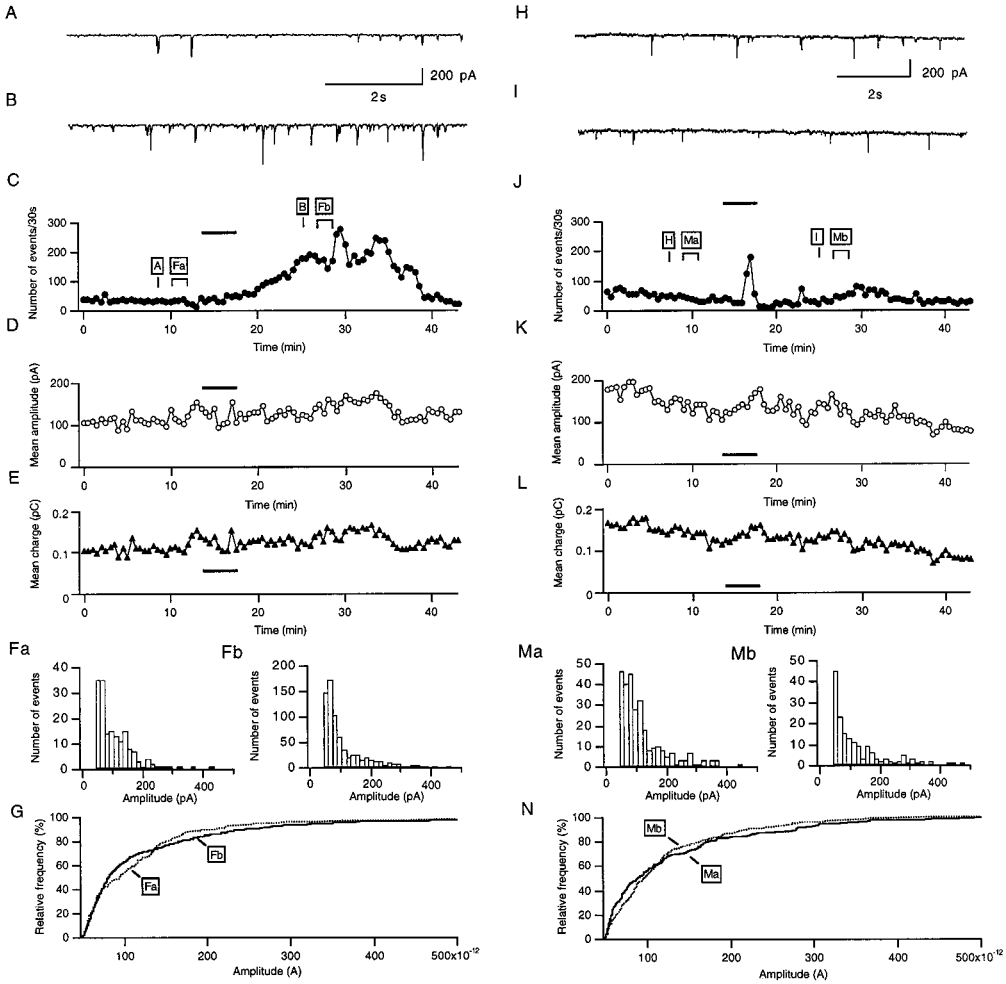

Figure 5. Hydrogen peroxide enhances inhibitory synaptic activity in wild-type (*A–G*), but not $Prnp^{0/0}$ (*H–N*) mouse Purkinje cells. Samples of the continuous recording of inhibitory synaptic currents before (*A, H*) and after (*B, I*) bath perfusion with 0.01% H_2O_2 at time points indicated in *C* and *J*. *C* and *J* show plots of the number of sIPSCs detected in 30 sec sample intervals as a function of time. The *bar* indicates the time of H_2O_2 application. *D* and *K*, as well as *E* and *L*, show the mean amplitudes and the mean charge of sIPSCs, calculated for 30 sec intervals, as a function of time. *F* and *M* show the amplitude histograms for the time periods (2.5 min) indicated in *C* and *J*. *G* and *N* show the cumulative amplitude distributions of the histograms shown in *F* and *M*. No shift in the amplitude distribution was observed in either the wild type (*G*) or $Prnp^{0/0}$ (*N*). The holding potential was −70 mV in this and all experiments shown in the following figures.

after addition of 0.01% H_2O_2 to the external solution. The application led to a marked enhancement of synaptic activity in wild-type mice (*B*), whereas there was no comparable effect in $Prnp^{0/0}$ mice (*I*). The time course of the H_2O_2 effect on the sIPSC frequency, mean amplitude, and mean charge is shown in *C–E* for the wild-type Purkinje cells and in *J–L* for the $Prnp^{0/0}$ mice Purkinje cells. In wild-type mice, the enhancement of the sIPSC frequency after the application of H_2O_2 (0.01%) develops progressively, reaching a peak value 15 min after the application has been seeded (Fig. 5*C*). In $Prnp^{0/0}$ mice, the sIPSC increases only very transient during the H_2O_2 application and decays during the following 10 min to values slightly lower than the frequency before the application (Fig. 5*J*).

The plots of the mean IPSC amplitude (Fig. 5*D*) and the mean charge (*E*) showed no significant effect of H_2O_2 in wild-type mice on these parameters. In the $Prnp^{0/0}$ mouse Purkinje cell, the mean IPSC amplitude and charge decreases slightly (*K*, *L*).

No significant changes were observed when comparing the amplitude histograms of the IPSCs (Fig. 5*F*,*M*) and the cumulative amplitude distributions (*G*, *N*) recorded from equivalent time periods (2.5 min), as indicated in Figure 5, *C* and *J*, before the application of H_2O_2 (*Fa*, *Ma*) and 10 min after the application of H_2O_2 (*Fb*, *Mb*).

Given that the major effect of H_2O_2 is an increase in the frequency of synaptic events, a presynaptic mechanism is very likely involved. It was therefore of interest to determine whether this effect could be observed in the absence of Na^+-dependent spikes in presynaptic neurons. In Purkinje cells studied here, the addition of TTX (0.5 μM) to the extracellular fluid did not alter the increase of miniature IPSCs (mIPSCs) after treatment with H_2O_2 (255 ± 53% of the basal frequency; $n = 4$). Because H_2O_2 increases the frequency of mIPSCs, this might result from an increased multiquantal release of transmitter caused by the discharge of Ca^{2+} spikes in the presynaptic inhibitory neurons. Experiments were therefore performed under conditions designed to eliminate Ca^{2+} entry. However, a similar increase in mIPSC frequency (215 ± 43%; $n = 4$) was observed in experiments in which Ca^{2+} was omitted from saline containing TTX and 200 μM EGTA.

No significant differences were observed in the resting membrane potentials and input resistances of Purkinje cells from $Prnp^{0/0}$ and wild-type mice, as described previously (Herms et al., 1995). H_2O_2 in the concentration used in this study was found to have no effect on either parameter, similar to the observation made by Pellmar et al.(1994) on hippocampal CA1 neurons. To elucidate whether there is a general alteration in $Prnp^{0/0}$ mouse synapses, which does not allow an increase of the sIPSC frequency because of a presynaptic stimulus, we studied the effect of the adenylyl cyclase activator forskolin. This is known to increase sIPSC, as well as mIPSC, frequency (Llano and Gerschenfeld, 1993). With the application of 10 μM forskolin, a similar increase of sIPSC frequency in both wild-type mice and $Prnp^{0/0}$ mice was observed (170 ± 50% compared with 165 ± 48% in $Prnp^{0/0}$ mouse Purkinje cells; $n = 4$).

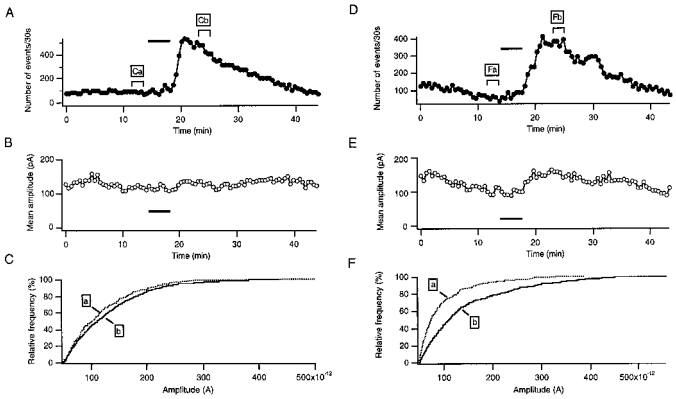

Figure 6. Hydrogen peroxide enhances inhibitory synaptic activity in two lines of Prnp-reconstituted $Prnp^{0/0}$ mice. PrP^C is overexpressed in all neurons in tg35 mice (*A–C*) and in all neurons except Purkinje cells in tg20 mice (*D–F*). *A*, *D*, Plots of the sIPSC frequency in 30 sec sample intervals against time in tg35 (*A*) and tg20 (*D*) mice. The *bar* indicates the time of H_2O_2 application. *B*, *E*, Plots of the mean sIPSCs amplitude, calculated for 30 sec intervals, as a function of time in tg35 (*B*) and tg20 (*E*) mice. *C*, *G*, Cumulative amplitude distributions for the time periods indicated in *A* and *B*. Whereas in tg35 (*C*) no significant shift can be observed, there is a shift to higher values in tg20 (*F*).

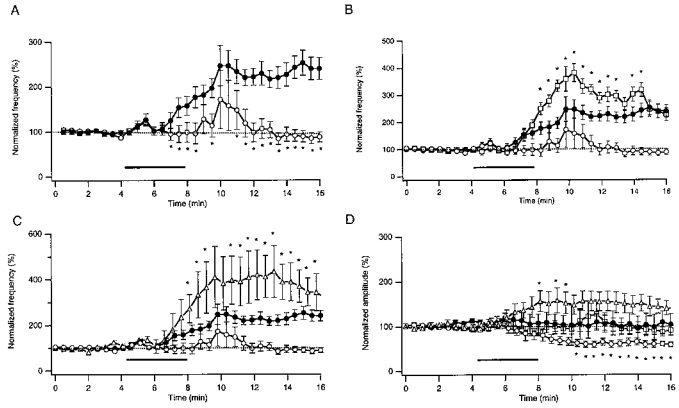

Figure 7. Pooled data of the effects of 0.01% H_2O_2 on the frequency and mean amplitude of Purkinje cell inhibitory synaptic currents in wild-type (●), $Prnp^{0/0}$ (○), tg35 (□), and tg20 (△) mice. Each point represents the mean ± SEM of frequency or amplitude of sIPSCs in 30 sec intervals normalized to the values before H_2O_2 application. Because of the tendency for amplitudes and frequencies of sIPSCs to decay slowly during the control period, only the last 3 min before the application were chosen for calculating the baseline (*broken line* at the 100% level). The threshold for detection of sIPSCs was set to −30 pA. *A*, Plots of the mean values of sIPSC frequency in wild-type ($n = 14$) and $Prnp^{0/0}$ ($n = 21$) mouse Purkinje cells, calculated for 30 sec intervals, as a function of time. The *bar* indicates the time during which H_2O_2 was applied. Significant differences between the two mouse strains are marked by *asterisks*. $p < 0.01$; *t* test. *B*, *C*, Plots of the mean values of the frequency of sIPSCs in tg35 (*B*; $n = 15$) and tg20 (*C*; $n = 4$) compared with wild-type and $Prnp^{0/0}$ mouse data. *D*, Plots of the mean sIPSC amplitudes normalized to values before H_2O_2 application in wild-type, $Prnp^{0/0}$, tg35, and tg20 mouse Purkinje cells. The amplitudes did not change in wild-type and tg35 cells after the application of H_2O_2. It increased slightly in tg20 mouse Purkinje cells and decreased significantly in $Prnp^{0/0}$ mouse cells.

To elucidate whether the differences observed between $Prnp^{0/0}$ and wild-type cells are caused by expression of PrP^C, we also examined transgenic mice, which overexpress PrP^C on a $Prnp^{0/0}$ background (tg35). Figure 6*A–C* shows a typical cell of a tg35 mouse. In Figure 6*A*, the sIPSC frequency, calculated for 30 sec intervals, is plotted as a function of time. As shown by the plot, the sIPSC frequency increased over sixfold when the response to H_2O_2 was maximal. No change in the mean sIPSC amplitude (Fig. 6*B*) or a significant shift in the cumulative amplitude distribution (Fig. 6*C*) were observed.

To elucidate whether the overexpression of PrP^C in either Purkinje cells or presynaptic neurons, i.e., stellate or basket cells, is the cause of the restored sIPSC frequency increase in PrP^C gene-reconstituted mice, we examined tg20 mice, which express PrP^C in cerebellar interneurons but not Purkinje cells (Fischer et al., 1996) and are therefore ideally suited for the distinction of presynaptic and postsynaptic effects when compared with $Prnp^{0/0}$ mice with no PrP^C expression at all and with tg35 and wild-type mice, which express PrP^C in interneurons and Purkinje cells as well. Figure 6*D–F* shows the response of a tg20 mouse Purkinje cell. The dramatic increase in the sIPSC frequency (Fig. 6*D*) after H_2O_2 application indicates that presynaptic PrP^C expression is important for the observed effect, whereas postsynaptic PrP^C does not seem to be necessary. The plot of the mean sIPSC amplitude (*E*) showed a small increase after H_2O_2 application, as well as a shift of the cumulative amplitude distribution to higher values (*F*), which indicates that H_2O_2 also modulates the sIPSC amplitude in tg20 mice.

Figure 7 illustrates cumulative data from 14 wild-type, 21 $Prnp^{0/0}$, 14 tg35, and 4 tg20 mouse Purkinje cells. In wild-type mice, the sIPSC frequency increased up to 250% of the level before H_2O_2 application (*A*). In $Prnp^{0/0}$ mice, the mean sIPSC frequency increased only transiently, resuming its initial level 5 min after H_2O_2 application (*A*). In tg35 Purkinje cells, which overexpress PrP^C on a $Prnp^{0/0}$ background, an increase of the sIPSC frequency was observed (*B*). Moreover this increase was significantly stronger than in wild-type mice, indicating that the amount of PrP^C expressed is critical for the effect of H_2O_2 on synaptic transmission. A similar increase of the sIPSC frequency was observed in tg20 mice (*C*). In wild-type and tg35 mice, the sIPSC amplitude was not altered by H_2O_2, whereas the mean values decreased in $Prnp^{0/0}$ mice. In tg20 mice, the mean sIPSC amplitude increased slightly after application of H_2O_2 (*D*).

DISCUSSION

Light microscopic studies on the cellular and subcellular location of PrP^C have yielded conflicting results. The majority of immunohistochemical investigations have indicated a somatic staining pattern of PrP^C (DeArmond et al., 1987; Piccardo et al., 1990; Safar et al., 1990; Bendheim et al., 1992; Manson et al., 1992a). In the cerebellum, a strong staining of Purkinje cell bodies, but not of the neuropil, has been described (DeArmond et al., 1987; Manson et al., 1992a). In contrast, using the histoblot technique, Taraboulos et al. (1992) found a neuropil staining pattern in hamster brain. The cerebellum was not examined in that study. More recently, an immunoelectron microscopic study (Fournier et al., 1995) demonstrated colocalization of PrP^C with the presynaptic vesicle protein synaptophysin, which led to the speculation that PrP^C might be a constituent of the synaptic vesicle membrane or a product stored within vesicles. Also, Salès et al. (1998) described synaptic staining in hamster brain using a highly sensitive free-floating immunohistochemical procedure. However, the electron microscopic data did not give convincing evidence of a preferential expression of PrP^C at the synaptic membrane because the tissue preservation in that study was not of sufficient quality as a result of the preembedding staining technique that was used. On the functional level, previous physiolog-

ical data on $Prnp^{0/0}$ mice have also yielded contradictory results concerning the direct involvement in the synaptic function of PrP^C (Collinge et al., 1994; Herms et al., 1995; Manson et al., 1995; Whittington et al., 1995; Lledo et al., 1996).

For a clarification of these questions, we performed biochemical, immunohistochemical, and electrophysiological experiments using various mouse lines. All investigations were performed on wild-type, PrP^C gene-ablated ($Prnp^{0/0}$), and PrP^C gene-reconstituted $Prnp^{0/0}$ (tg20 and tg35) mice. Because these transgenic lines differ in their expression pattern of PrP^C, they were particularly suitable for our experiments. Tg35 mice express PrP^C in all neurons, whereas tg20 mice express PrP^C in all neurons except Purkinje cells (Fischer et al., 1996). These mice are therefore ideal for a functional analysis of presynaptic and postsynaptic factors in the synaptic transmission of Purkinje cells depending on the PrP^C expression.

The histoblot data of PrP^C-overexpressing mice presented here clearly show that PrP^C immunostaining is most intense in regions of dense neuropil, such as the stratum radiatum and stratum oriens of the CA1 region, and is virtually absent from the granule cell layer of the dentate gyrus and the pyramidal cell layer throughout the Ammon's horn. Immunohistochemistry of the retina shows the predominant location of PrP^C in regions of high synaptic density, such as the inner and outer plexiform layers. The observed colocalization of PrP^C with the synaptic vesicle protein synaptophysin in the inner and outer plexiform layers is another strong indication of the synaptic location of PrP^C.

Immunohistochemistry had not shown detectable levels of PrP^C in the brains of wild-type mice. Therefore, a Western blot analysis of synaptic fractions of wild-type mouse brains was performed and was compared with preparations of PrP^C-overexpressing transgenic animals. PrP^C was found to be enriched in the synaptic plasma membrane fraction in both wild-type and PrP^C-overexpressing mice. This was similar to the distribution of other synaptic proteins, such as synaptotagmin and the NMDA-R1 receptor subunit. In contrast to the synaptic vesicle protein synaptotagmin, which is more strongly enriched in the synaptic vesicle fraction than in the synaptic plasma membrane fraction, PrP^C was more strongly enriched in the synaptic plasma membrane fraction, indicating that a predominant location of PrP^C on the synaptic vesicle membrane as supposed recently (Fournier et al., 1995) does not seem very likely. Also, the finding that trypsinization of synaptosomes leads to a complete degradation of PrP^C while a synaptic vesicle protein remains intact further supports the notion that PrP^C is predominantly, if not exclusively, located on the surface of the synaptic plasma membrane.

On the functional level, our previous electrophysiological investigations of inhibitory and excitatory synaptic transmission in the cerebellum of $Prnp^{0/0}$ mice did not support the notion that PrP^C is involved in synaptic transmission under normal conditions (Herms et al., 1995). The findings we present here indicate that prominent differences in synaptic transmission between wild-type and $Prnp^{0/0}$ mice can be observed in certain biochemically defined conditions. The key result of our experiments is that bath application of H_2O_2 induces a strong and sustained increase in the frequency of sIPSCs in Purkinje cells of normal mice but not of $Prnp^{0/0}$ mice. In transgenic mouse strains in which the prion protein gene had been reintroduced on a $Prnp^{0/0}$ background, i.e., tg 35 and tg20 (PrP^C gene-reconstituted mice), all tested cells presented a strong and lasting increase of sIPSC frequency after H_2O_2 application. Therefore, the effect elicited by hydrogen peroxide is not unspecific but is related to PrP^C expression in these animals (functional reconstitution). The fact that the increase in sIPSC frequency was also observed in Purkinje cells of tg20 mice, which have been shown to overexpress PrP^C in neuronal cells excluding Purkinje cells, gives strong evidence that it is the expression on the presynaptic plasma membrane of the interneuron that is responsible for the observed differences in the response to H_2O_2 in the different transgenic lines.

How is the effect of H_2O_2 related to PrP^C expression? We propose that the different H_2O_2 responses of wild-type, $Prnp^{0/0}$, and transgenic mice that overexpress PrP^C (tg20 and tg35) are caused by the different amounts of copper located at the presynaptic plasma membrane. Metal ions, i.e., copper and iron, decompose H_2O_2 to highly reactive oxygen radicals at the site at which the metal ions are located (Halliwell, 1992). At the synapse, these radicals alter synaptic vesicle release through an increase in the presynaptic calcium concentration (Pellmar et al., 1994; Pellmar, 1995) probably because of an alteration of intracellular calcium pools that are located close to the presynaptic membrane. Because an increase in the free calcium concentration at the presynaptic membrane is known to increase the probability of synaptic vesicle release (Heidelberger et al., 1994), this is the most likely explanation for the observed sIPSC and mIPSC frequency increase after the application of H_2O_2 in wild-type mouse cerebellar Purkinje cells of the present study. The sIPSC frequency increase after the application of H_2O_2 is significantly lower in $Prnp^{0/0}$ mice in which the amount of copper was found to be reduced in synaptosomes than in wild-type mice. In the transgenic mice in which PrP^C had been reintroduced, however, both the synaptosomal copper content and the H_2O_2 effect on sIPSC frequency were found to be rescued.

Also, the IPSC amplitude was found to be altered by H_2O_2 application, but only in $Prnp^{0/0}$ mice and the transgenic mice, which highly overexpress PrP^C on the presynaptic side (tg20). Although a decrease of the IPSC amplitude was observed in $Prnp^{0/0}$ mice compared with wild-type mice, an increased was found in the transgenic mice that overexpress PrP^C on the presynaptic side. Because tg20 mice do not express PrP^C in Purkinje cells, these two mouse lines differ only in the PrP^C expression on the presynaptic side of the interneuron–Purkinje cell synapse. A presynaptic cause therefore seems very likely.

However, copper-binding by PrP^C at the presynaptic plasma membrane is probably not the only cause of the observed differences in the synaptosomal copper content of wild-type and $Prnp^{0/0}$ mice. Synaptosomes include the presynaptic plasma membrane, as well as parts of the postsynaptic plasma membrane, and they also include high amounts of presynaptic cytosol and organelles such as mitochondria. Considering that several proteins in synaptosomes bind copper, the observed reduction of 50% in the copper concentration of $Prnp^{0/0}$ mouse synaptosomes is too high to be only caused by a loss of copper that is bound to PrP^C. Indeed, we suppose that the copper bound to PrP^C contributes only very little to the overall copper content measured in synaptosomes. This is supported by the finding that the transgenic line that overexpresses PrP^C (tg20) shows an increased response to H_2O_2 compared with wild-type mice but does not show a higher synaptosomal copper concentration.

It therefore seems that the strong differences in the synaptosomal copper content of $Prnp^{0/0}$ and wild-type mice are caused by an alteration of copper uptake into synaptosomes by loss of PrP^C. Our working hypothesis is that PrP^C recaptures copper that is released into the synaptic cleft by synaptic vesicle fusion (Hartter

and Barnea, 1988). In $Prnp^{0/0}$ mice, copper is lost into the extracellular space and cannot be taken up as effectively into the presynaptic cytosol in which the copper content is lastingly reduced. This may be the cause of the reduced activity of a cytosolic copper-dependent enzyme, the superoxide dismutase, observed in $Prnp^{0/0}$ mice (Brown et al., 1997b).

In addition, the loss of copper binding at the synaptic cleft through the loss of PrP^C at the synaptic membrane, which might lead to a slightly higher copper concentration in the extracellular fluid in $Prnp^{0/0}$ mice, may well be a relevant factor in explaining alterations in the properties of the $GABA_A$ receptor, as well as in hippocampal long-term potentiation (LTP), as has been described for $Prnp^{0/0}$ mice (Collinge et al., 1994; Manson et al., 1995; Whittington et al., 1995). The $GABA_A$ receptor, as well as long-term potentiation in the hippocampus, have been shown recently to be affected by copper concentrations of only 0.1–1 μM (Doreulee et al., 1997; Sharonova et al., 1998). Therefore, minor differences in the extracellular copper concentration would cause alterations of the $GABA_A$ receptor and of LTP. Because the physiological constitution of the extracellular fluid using brain slices in electrophysiological experiments may vary considerably, differences in the experimental setup, such as slice thickness, the position of the cell in the studied slice, the buffer used, and, in particular, higher temperatures with increased oxidative stress, quite clearly influence results, depending on the amount of PrP^C and copper present in the synapse in wild-type and $Prnp^{0/0}$ animals. Such differences may therefore explain why an alteration of the $GABA_A$ receptor, as well as a diminished LTP in $Prnp^{0/0}$ mouse neurons, was not reproduced by other observers using slightly different protocols, including lower temperatures (Herms et al., 1995; Lledo et al., 1996).

In conclusion, morphological and biochemical investigations of different PrP^C-transgenic mouse lines provide strong evidence of a predominantly synaptic location of PrP^C. Electrophysiological studies indicate that PrP^C is a prominent copper-binding protein at the presynaptic plasma membrane. Loss of PrP^C in $Prnp^{0/0}$ mice strongly affects the copper content in synaptosomes, indicating that PrP^C is involved in synaptic copper homeostasis. The exact function of copper binding by PrP^C at the synaptic plasma membrane and its role in synaptic copper metabolism, as well as in synaptic transmission, remain to be clarified.

REFERENCES

Bendheim PE, Brown HR, Rudelli RD, Scala LJ, Goller NL, Wen GY, Kascsak RJ, Cashman NR, Bolton DC (1992) Nearly ubiquitous tissue distribution of the scrapie agent precursor protein. Neurology 42:149–156.

Brose N, Halpain S, Suchanek C, Jahn R (1989) Characterization and partial purification of a chloride- and calcium-dependent glutamate-binding protein from rat brain. J Biol Chem 264:9619–9625.

Brose N, Huntley GW, Stern-Bach Y, Sharma G, Morrison JH, Heinemann SF (1994) Differential assembly of coexpressed glutamate receptor subunits in neurons of rat cerebral cortex. J Biol Chem 269:16780–16784.

Brown DR, Qin K, Herms JW, Madlung A, Manson J, Strome R, Fraser P, Kruck T, von Bohlen A, Schulz-Schaeffer W, Giese A, Westaway D, Kretzschmar H (1997a) The cellular prion protein binds copper *in vivo*. Nature 390:684–687.

Brown DR, Schulz-Schaeffer WJ, Schmidt B, Kretzschmar HA (1997b) Prion protein-deficient cells show altered response to oxidative stress due to decreased SOD-1 activity. Exp Neurol 146:104–112.

Büeler H, Fischer M, Lang Y, Bluethmann H, Lipp H-P, DeArmond SJ, Prusiner SB, Aguet M, Weissmann C (1992) Normal development and behaviour of mice lacking the neuronal cell-surface PrP protein. Nature 356:577–582.

Carlin RK, Grab DJ, Cohen RS, Siekevitz P (1980) Isolation and characterization of postsynaptic densities from various brain regions: enrichment of different types of postsynaptic densities. J Cell Biol 86:831–843.

Collinge J, Whittington MA, Sidle KCL, Smith CJ, Palmer MS, Clarke AR, Jefferys JGR (1994) Prion protein is necessary for normal synaptic function. Nature 370:295–297.

DeArmond SJ, Mobley WC, DeMott DL, Barry RA, Beckstead JH, Prusiner SB (1987) Changes in the localization of brain prion proteins during scrapie infection. Neurology 37:1271–1280.

Doreulee N, Yanovsky Y, Haas HL (1997) Suppression of long-term potentiation in hippocampal slices by copper. Hippocampus 7:666–669.

Edwards FA, Konnerth A, Sakmann B, Takahashi T (1989) A thin slice preparation for patch-clamp recordings from neurones of the mammalian central nervous system. Pflügers Arch 414:600–612.

Fischer M, Rülicke T, Raeber A, Sailer A, Moser M, Oesch B, Brandner S, Aguzzi A, Weissmann C (1996) Prion protein (PrP) with amino-proximal deletions restoring susceptibility of PrP knockout mice to scrapie. EMBO J 15:1255–1264.

Fournier J-G, Escaig-Haye F, De Villemeur TB, Robain O (1995) Ultrastructural localization of cellular prion protein (PrP^C) in synaptic boutons of normal hamster hippocampus. C R Acad Sci III 318:339–344.

Gilman SC, Bonner MJ, Pellmar TC (1992) Peroxide effects on [H-3]L-glutamate release by synaptosomes isolated from the cerebral cortex. Neurosci Lett 140:157–160.

Groschup MH, Langeveld J, Pfaff E (1994) The major species specific epitope in prion proteins of ruminants. Arch Virol 136:423–431.

Halliwell B (1992) Reactive oxygen species and the central nervous system. J Neurochem 59:1609–1623.

Hamill O, Marty A, Neher E, Sakmann B, Sigworth FJ (1981) Improved patch-clamp techniques for high resolution current recording from cells and cell-free membrane patches. Pflügers Arch 391:85–100.

Hartter DE, Barnea A (1988) Evidence for release of copper in the brain: depolarization-induced release of newly taken-up ^{67}copper. Synapse 2:412–415.

Heidelberger R, Heinemann C, Neher E, Matthews G (1994) Calcium dependence of the rate of exocytosis in a synaptic terminal. Nature 371:513–515.

Herms JW, Kretzschmar HA, Titz S, Keller BU (1995) Patch-clamp analysis of synaptic transmission to cerebellar Purkinje cells of prion protein knockout mice. Eur J Neurosci 7:2508–2512.

Huttner WB, Schiebler W, Greengard P, De Camilli P (1983) Synapsin I (protein I), a nerve terminal-specific phosphoprotein. III. Its association with synaptic vesicles studied in a highly purified synaptic vesicle preparation. J Cell Biol 96:1374–1388.

Kitamoto T, Shin R-W, Doh-ura K, Tomokane N, Miyazono M, Muramoto T, Tateishi J (1992) Abnormal isoform of prion proteins accumulates in the synaptic structures of the central nervous system in patients with Creutzfeldt-Jakob disease. Am J Pathol 140:1285–1294.

Krasemann S, Groschup M, Hunsmann G, Bodemer W (1996) Induction of antibodies against human prion proteins (PrP) by DNA-mediated immunization of PrP0/0 mice. J Immunol Methods 199:109–118.

Kretzschmar HA, Prusiner SB, Stowring LE, DeArmond SJ (1986) Scrapie prion proteins are synthesized in neurons. Am J Pathol 122:1–5.

Llano I, Gerschenfeld HM (1993) β-adrenergic enhancement of inhibitory synaptic activity in rat cerebellar stellate and Purkinje cells. J Physiol (Lond) 468:201–224.

Llano I, Marty A, Armstrong CM, Konnerth A (1991) Synaptic- and agonist-induced excitatory currents of Purkinje cells in rat cerebellar slices. J Physiol (Lond) 434:183–213.

Lledo PM, Tremblay P, DeArmond SJ, Prusiner SB, Nicoll RA (1996) Mice deficient for prion protein exhibit normal neuronal excitability and synaptic transmission in the hippocampus. Proc Natl Acad Sci USA 93:2403–2407.

Manson J, McBride P, Hope J (1992a) Expresson of the PrP gene in the brain of *sinc* congenic mice and its relationship to the development of scrapie. Neurodegeneration 1:45–52.

Manson J, West JD, Thomson V, McBride P, Kaufman MH, Hope J (1992b) The prion protein gene: a role in mouse embryogenesis? Development 115:117–122.

Manson JC, Hope J, Clarke AR, Johnston A, Black C, MacLeod N (1995) PrP gene dosage and long term potentiation. Neurodegeneration 4:113–115.

McMahon HT, Foran P, Dolly JO, Verhage M, Wiegant V, Nicholls DG (1992) Tetanus toxin and botulinum toxins type A and B inhibit glutamate, γ-aminobutyric acid, aspartate, and metenkephalin release from synaptosomes. Clues to the locus of action. J Biol Chem 267:21338–21343.

Moser M, Colello RJ, Pott U, Oesch B (1995) Developmental expression of the prion protein gene in glial cells. Neuron 14:509–517.

Palmeira CM, Santos MS, Carvalho AP, Oliveira CR (1993) Membrane lipid peroxidation induces changes in γ-[^{3}H]aminobutyric acid transport and calcium uptake by synaptosomes. Brain Res 609:117–123.

Pellmar TC (1995) Use of brain slices in the study of free-radical actions. J Neurosci Methods 59:93–98.

Pellmar TC, Gilman SC, Keyser DO, Lee KH, Lepinski DL, Livengood D, Meyers Jr LS (1994) Reactive oxygen species on neural transmission. Ann NY Acad Sci 738:121–129.

Perin MS, Fried VA, Mignery GA, Jahn R, Südhof TC (1990) Phospholipid binding by a synaptic vesicle protein homologous to the regulatory region of protein kinase C. Nature 345:260–263.

Piccardo P, Safar J, Ceroni M, Gajdusek DC, Gibbs Jr CJ (1990) Immunohistochemical localization of prion protein in spongiform encephalopathies and normal brain tissue. Neurology 40:518–522.

Prusiner SB, Telling G, Cohen FE, DeArmond SJ (1996) Prion diseases of humans and animals. Semin Virol 7:159–173.

Safar J, Ceroni M, Piccardo P, Liberski PP, Miyazaki M, Gajdusek DC, Gibbs Jr CJ (1990) Subcellular distribution and physicochemical properties of scrapie-associated precursor protein and relationship with scrapie agent. Neurology 40:503–508.

Salès N, Rodolfo K, Hässig R, Faucheux B, Di Giamberardino L, Moya KL (1998) Cellular prion protein localization in rodent and primate brain. Eur J Neurosci 10:2464–2471.

Sharonova IN, Vorobjev VS, Haas HL (1998) High-affinity copper block of $GABA_A$-receptor-mediated currents in acutely isolated cerebellar Purkinje cells of the rat. Eur J Neurosci 10:522–528.

Stahl N, Borchelt DR, Hsiao K, Prusiner SB (1987) Scrapie prion protein contains a phospatidylinositol glycolipid. Cell 51:229–240.

Taraboulos A, Jendroska K, Serban D, Yang S-L, DeArmond SJ, Prusiner SB (1992) Regional mapping of prion proteins in brain. Proc Natl Acad Sci USA 89:7620–7624.

Whittington MA, Sidle KCL, Gowland I, Meads J, Hill AF, Palmer MS, Jefferys JGR, Collinge J (1995) Rescue of neurophysiological phenotype seen in PrP null mice by transgene encoding human prion protein. Nat Genet 9:197–207.